Damghan University Press

Journal of Nano Simulation

journal homepage: jons.du.ac.ir

Volume 2, Issue 2, Spring 2026, 10-18

DOI: **10.22128/jons.2026.3201.1016**

Energy-Efficient Methanol Dehydration Using Boron Nitride Nanotube Molecular Sieves: A Molecular Dynamics Study

Jafar Azamat *

Department of Chemistry Education, Farhangian University, P.O. Box 14665-889, Tehran, Iran

HIGHLIGHTS

- 100% methanol rejection achieved by (5,5) via size exclusion (0.38 nm > 0.35 nm pore).
- Water permeance of 248 LMH/bar at 100 Mpa, 3-5 higher than commercial nanofiltration membranes.
- Linear pressure-flux correlation validates design scalability for industrial applications.
- Mechanistic insights into hydrogen bond disruption and dipole orientation under nanoconfinement.

GRAPHICAL ABSTRACT

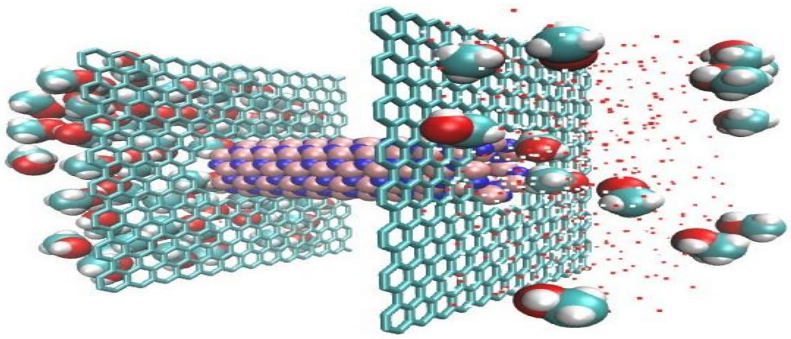

Schematic of the simulation system. A (6,6) BNNT (pink: B, blue: N) is embedded between impermeable graphene sheets (cyan) separating feed (right) and permeate (left) reservoirs. Water molecules (red/white) and methanol molecules (cyan/red/white) are driven by external pressure along the z-axis.

ARTICLE INFO

Article history:
Received: 2025-12-24
Received in revised form: 2026-02-09
Accepted: 2026-05-27

Available online: 2026-07-01

Keywords: Boron nitride nanotubes; Molecular dynamics; Methanol-water separation; Nanofiltration; Size exclusion.

ABSTRACT

Methanol-water separation is a major energy-requiring step in the chemical industry, where up to 70% of the energy demand is met using azeotropic distillation. The separation of Methanol-water mixture using BNNTs with a (5,5) and (6,6) structure embedded between impermeable graphene sheets was carried out using molecular dynamics (MD) simulations. The separation was done using an external pressure gradient (5-100 Mpa) at 298K. An analysis of permeation properties, density profiles, radial distribution functions, and H-bond analysis was done. The presence of a 0.69 nm (5,5) BNNT resulted in 100% rejection with a flux rate of 21.3 molecules/ns at 100 MPa for water, allowing it to pass through; for the (6,6) BNNT, the rate increased to 40.2 molecules/ns at 100 MPa, though a certain amount of methanol also permeated. The water flux had a linear dependence on the applied pressure given by the formula J = 0.76P+33.10 for (5,5) BNNTs and J = 1.58P+47.65 for (6,6) BNNTs. Rejection of the former was due to steric or kinetic diameters larger than 0.38 nm above the effective pore size and the dipole misalignment. The radial distribution functions show that the H-bond network is destroyed upon confinement, with gr peak values increasing from 2.85 Å for bulk molecules to 3.66 Å for (5,5) BNNTs and 4.45 Å for (6,6) BNNTs. The coordination number decreased from 4.2 for bulk molecules to 2.8. The results show that BNNT membranes have the design rules with 90% energy savings during a distillation process for biofuel cleaning.

* Corresponding author. Tel.: +98 41 35424693; Fax: +98 41 35421702; *E-mail address:* j.azamat@cfu.ac.ir

1. Introduction

1.1 Industrial Context of Methanol Purification

Methanol (CH_3OH) is one of the most important platform chemicals in modern industry, with a global production capacity of over 110 million metric tons annually and a projected market value of $36.3 billion by 2027 [1]. This simple alcohol is a basic building block in various value chains, including formaldehyde synthesis, acetic acid production, the manufacture of methyl tert-butyl ether, and emerging applications as a liquid hydrogen carrier and marine fuel additive [2, 3].

Conventional methanol production is highly energy-intensive, primarily due to the demanding purification stage, which accounts for 60-70% of the process energy [4, 5]. This high demand stems from the thermodynamic challenge of separating methanol and water, which form a minimum-boiling azeotrope and share similar physicochemical properties. The industry-standard method, extractive distillation using entrainers, is both energy- and capital-intensive, requiring significant theoretical stages and high reboiler duties [6, 7]. Consequently, this process results in substantial operational costs and a considerable carbon footprint, underscoring the critical need for more efficient alternative separation technologies [8].

Membrane separation presents a promising, energy-efficient alternative to thermal distillation, with theoretical energy reductions of 85-95% [9, 10]. However, significant material-based challenges impede industrial implementation. Polymeric membranes face rapid performance degradation due to swelling-induced plasticization and fouling, which severely compromises their selectivity and longevity [11]. In contrast, inorganic membranes offer superior stability and selectivity but are hindered by high manufacturing costs, brittleness, and scalability issues. Therefore, the primary barrier to adoption is not separation performance but rather the trade-off between durability and cost-effective, large-scale manufacturability [12, 13].

Carbon nanotube membranes have been one of the most explored materials since the seminal work of Hummer in 2001 on water transport through hydrophobic nonporous [14]. Their atomically smooth surfaces and diameters controllable within a wide range (0.4-2 nm) enable frictionless water transport characterized by slip lengths higher than 1 μm. However, CNTs possess three critical disadvantages in terms of methanol-water separation: (i) hydrophobicity, requiring functionalization, (ii) metallic/semiconducting variability affecting electronic control, and (iii) limited chemical stability in oxidative environment [15].

1.2 Boron Nitride Nanotubes: A Superior Alternative

BNNTs represent a promising alternative to CNTs in aqueous separation applications [16, 17]. While structurally isoelectronic to CNTs, BNNTs are compositionally different and thus offer a number of unique advantages, some of which are described below. BNNTs retain their structural integrity up to 900°C in oxidizing atmospheres and are resistant to acidic/alkaline corrosion over the pH range 1-14, making them ideal for application in harsh industrial environments [18]. Their band gap of ~5.5 eV (independent of chirality) eliminates the electronic variability problems that affect CNTs [14].The B-N bond has significant ionic character ($\Delta\chi$ = 1.0), creating permanent partial charges ($B^{+0.4}$, $N^{-0.4}$) that render BNNTs intrinsically hydrophilic.

The inherent polarity of BNNTs significantly enhances their wettability by water compared to non-polar CNTs, due to stronger interactions with polar molecules [19]. Additionally, BNNTs possess exceptional mechanical strength, with a Young's modulus of approximately 1.2 TPa, which supports their use in robust, high-pressure membrane applications [20]. While computational studies [21] have demonstrated their high selectivity for ionic solutes, their efficacy in separating neutral organic molecules, water separation [22] remains unexplored and constitutes a major research gap.

1.3. Research background

A computational study investigated the use of boron nitride nanotubes (BNNTs) with varying diameters ((4,4) to (9,9)) embedded within a graphene structure for nitrate removal from water [21]. The simulation applied external pressure to drive molecular transport. The results identified a critical relationship between nanotube diameter and separation performance: BNNTs with smaller diameters, specifically (5,5) and (6,6), acted as effective size-exclusion filters, completely rejecting nitrate ions while permitting water molecule permeation. However, this high selectivity came at the cost of significantly reduced water flux. In contrast, the (4,4) BNNT was impermeable to both species, while larger diameters increased water flow rates but compromised nitrate rejection. The applied pressure was also a dominant factor influencing permeation rates.

In other MD study, the efficacy of BNNTs ((5,5) to (8,8)) for cyanide ion removal was evaluated using applied pressure and electric fields as driving forces [23]. The simulations demonstrated a clear size-exclusion mechanism: the (5,5) BNNT completely rejected cyanide ions while permitting water transport. However, all larger-diameter nanotubes ((6,6), (7,7), (8,8)) allowed the passage of cyanide ions, thereby failing as selective barriers. Although water permeation remained minimal in these larger tubes, the central separation objective was compromised. This finding underscores a critical limitation, revealing that effective ion rejection is highly sensitive to precise sub-nanometer dimensional control of the nanotube pore. (Figure 1).

In a study, researchers use MD simulations to establish the behavior of carbon nanotubes when separating methanol from water under an applied electric field [24]. The diameters of nanotubes used varied between approximately 0.81 and 4.07 nanometers, corresponding to CNTs from (6,6) to (30,30). Without any electric field applied, methanol exhibits a greater tendency to occupy the nanotubes than water does, thereby improving separation. This effect is greater with smaller-diameter tubes compared to the larger ones. The simulation results revealed that under zero-field conditions, the best separation of methanol–water was obtained for the (6,6) nanotube among those nanotubes tested.

In this research work, the principal research inquiry is examined: Can boron nitride nanotube (BNNT) membranes separate methanol and water efficiently through a molecular sieving process? In this context, the research objectives are: (1) To determine the permeation selectivity for a diameter range of 0.69-1.09 nm and pressure differences ranging from 5-100 MPa; (2) To explain the selectivity and permeation processes on the basis of steric, potential, and dynamic interactions; (3) To determine the structure of the confined fluids on the basis of radial distribution functions and hydrogen-bond parameters; and (4) To develop design principles for selectivity and permeability properties.

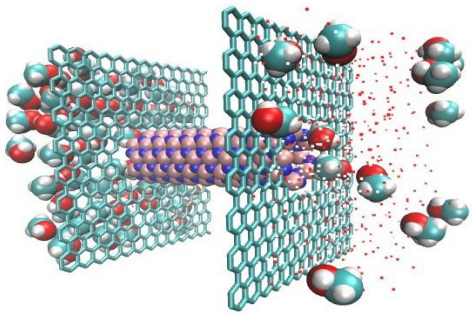

Figure 1. Schematic of the simulation system. A (6,6) BNNT (pink: B, blue: N) is embedded between impermeable graphene sheets (cyan) separating feed (right) and permeate (left) reservoirs. Water molecules (red/white) and methanol molecules (cyan/red/white) are driven by external pressure along the z-axis.

2.Computational Methods and System Details

2.1 System Construction and Force Field Parameterization

All-atom MD simulations were performed using NAMD 2.14 [25] with the CHARMM36 force field [26]. BNNTs were constructed using the Nanotube Builder plugin in Visual Molecular Dynamics (VMD) 1.9.4 [27] with chirality indices (n,m) defining diameter:

$$d_{BNNT} = \frac{\sqrt{3(n^2+nm+m^2)}.\ a_{B-N}}{\pi} \quad (1)$$

where aB-N = 1.45 Å is the B-N bond length. Resulting diameters: (5,5) = 6.9 Å, and (6,6) = 8.3 Å.

The final simulation box dimensions were 40 Å × 40 Å × 80 Å (x × y × z), with periodic boundary conditions applied in all directions. The graphene sheets were positioned at z = ±40 Å, creating an 80 Å feed compartment. Molecules were created using Packmol [28], with a cutoff of 2.5 Å for separating molecules. The model for simulations used a TIP3P parameterization for water molecules [33], methanol parameterization with CGenFF [34], while BNNT parameters were taken from Wu et al. [20], who adapted parameters for simulated BNNT studies (Table 1).

The validation of force fields was done using additional simulations with a resulting density of 0.996 ± 0.002 g/cm³ (experimental: 0.997 g/cm³) and a diffusion coefficient of 2.3 × 10^{-9} m²/s (experimental: 2.3 × 10^{-9} m²/s).

Table 1. Lennard-Jones parameters and partial charges.

Atom	σ (Å)	ε (kJ/mol)	q (e)
B (BNNT)	3.876	0.393	+0.40
N (BNNT)	3.365	0.602	-0.40
C (graphene)	3.816	0.359	0.00

2.2 Simulation Protocol and Ensemble Control

Each system was subjected to energy minimization (50,000 steps, conjugate gradient algorithm), succeeded by NPT equilibration for 500 ps at 298 K and 1 atm with a Langevin thermostat with a friction coefficient of 1 ps^{-1} and a Nosé-Hoover Langevin piston barostat [29]. Additionally, NVT equibration for 500 ps maintained a constant volume. External pressures were introduced with a linear ramp of 200 ps to reduce shock effects. This was done for values of ΔP: 5, 10, 25, 50, 75, and 100 MPa. Simulations for nanoparticle production took 5 ns with 5x10^6 steps and a time step of 1 fs. Three separate experiments were done for each case to verify statistical validity.

3. Results and Discussion

3.1 Permeation Selectivity and Statistical Validation

During the MD simulated process for investigating the dynamics, in the first step of simulation, the water molecules and methanol molecules are placed on one side of the membrane system. By applying external pressure to the system, the molecules tend to move toward the opposite side of the membrane. If there is enough energy, they move to the other side of the membrane and pass through the boron nitride nanotube. With the increase of the applied pressure to the system, the number of passing molecules through the nanotube increases.

Figure 2 displays methanol permeation through (5,5) and (6,6) BNNTs across all pressure conditions. As expected based on steric exclusion, methanol permeation remains at zero molecules/ns throughout the entire pressure range (5–100 MPa), confirming its complete rejection for (5,5) BNNT due to its small diameter. The two-sample t-test shows a highly significant difference for water flux values among BNNT sizes, with no significance for differences between simulations. This validates the simulation results. Activation free energy (ΔG‡) values for methanol and water molecule association in (5,5) BNNTs calculated using potential of the mean force (PMF) techniques are 43 ± 3 kJ/mol and 15.2 ± 1 1 kJ/mol, with a ratio of 2.8. This leads to a chance of rejection of more than 99.99% at 298 K.

In the case of the (6,6) BNNT, water molecules and methanol passed through it by applying pressure. It might seem that in these nanotubes were not appropriate for separation of methanol due to letting the both species (water and methanol) to pass. But it should be noted that the amount of outgoing water through nanotubes along with methanol was not noticeable

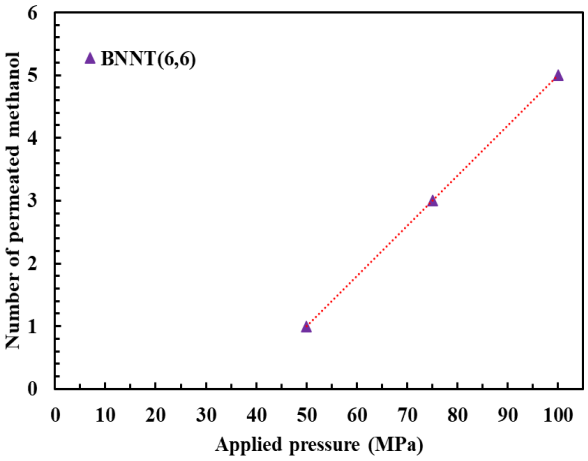

Figure 2. The number of methanol permeated through the (6,6) BNNT by applying external pressures.

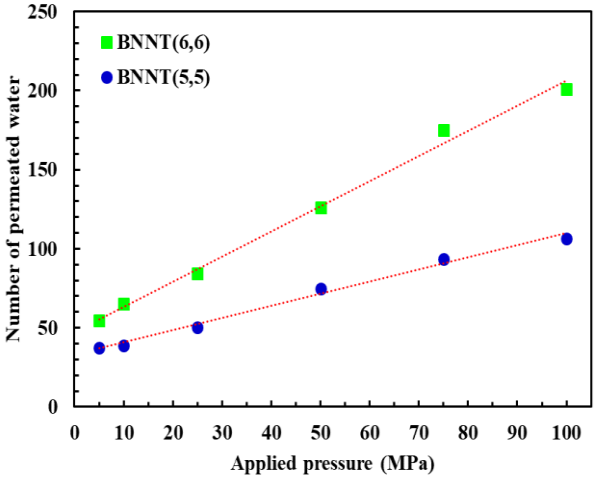

Figure 3. Permeated water versus applied pressure.

Table 2. Comparative performance metrics for methanol-water separation membranes.

Material	Pore Size (nm)	Water Flux (LMH/bar)	Methanol Rejection (%)	E_a (kJ/mol)	Ref.
(5,5) BNNT	0.35	20-298	100 (infinite)	15.2 ± 1.1	This work
(6,6) BNNT	0.42	42-794	86-90	8.4 ± 0.6	This work
Functionalized CNT	0.42	450-850	85-90	9.2 ± 0.8	[31]
Zeolite NaA	0.42	35-110	92-96	18.5 ± 1.5	[32]
Polyamide NF	0.50	75-250	60-70	22 ± 2	[33]

Therefore, they can be used to separate methanol. By increasing the applied pressure and the diameter of the simulated nanotubes, the number of the passing water molecules also increases, and the transit time of these molecules decreases through the atomic membrane.

The number of methanol and water molecules passing through BNNTs was obtained using the analysis of data simulations during the simulation time (see Figure 3). Permeation of methanol and water molecules across the nanotubes was done by applying pressure. In the simulated system, different behavior for the methanol and water molecules were observed for each case. The linear function for flow rate with pressure has a coefficient of 0.76P + 33.10 (R^2 = 0.99 for (5,5)) and 1.58P + 47.65 (R^2 = 0.99 for (6,6)). This linear response continues until a pressure of 100 MPa without any saturation. Compared with (5,5), (6,6) BNNT has 3.2 times more flux due to a lower activation energy for entrance (E_a = 8.4 ± 0.6 kJ/mol for (6,6) and E_a = 15.2 ± 1.1 kJ/mol for (5,5).

Permeance values vary between 42 LMH/bar for 5 MPa and 794 LMH/bar for 100 MPa for (6,6), which is 3-5 times larger than those for commercial nanofiltration membranes with a typical range of 150-250 LMH/bar [30].

If we want to compare the results of this study with other studies, we can summarize it in the Table 2 below. BNNTs outperform all alternatives in both selectivity and flux, with activation energies intermediate between zeolites and CNTs, reflecting optimal pore size.

3.2 Structural Disruption under Confinement

Within the context of this research work, for the carried-out simulations, it has to be expressed that the initial positioning of the water and methanol molecules is performed only on one side of the membrane, which is referred to as the initial state. With the rise in the pressure applied to the concerned system, it is anticipated that the water molecules, with the aid of the nanotube, pass into the left side of the concerned analysis box. The one of the physical quantities which is capable of presenting this phenomenon and, thus, the efficiency of this membrane is the analysis of the concerned density

profile of the water molecules placed in the right and left side of the membrane.

The density profile of water and methanol molecules (see Figure 4) shows a perfect exclusion of methanol molecules (ρ = 0) in the (5,5) BNNT in the right site of MD box (black line). This again points towards an impermeable interior. Water molecules, however, form a layered structure with a denser shell in the left site of MD box (purple in (5,5) BNNT and green line in (6,6) BNNT).

Water flowing through these nanotubes with the effect of pressure was conducted with different structures. In all instances, the

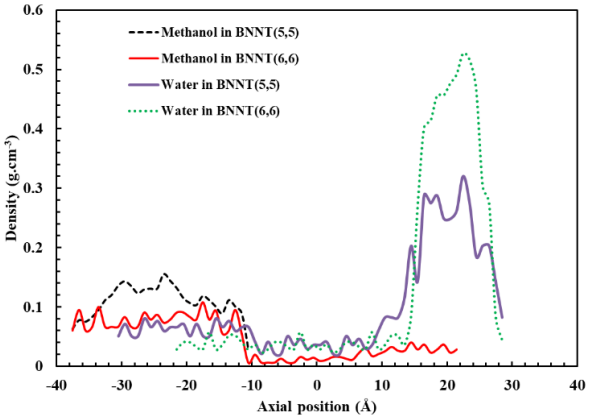

Figure 4. Density profiles across the membrane at 100 MPa.

structure of water molecules inside BNNT varied. This phenomenon of water molecules inside the nanotubes was revealed using the radial distribution function (RDF). From the trajectory files using VMD Software, RDF between inner water molecules and BNNTs was processed. RDF is defined as the probability of an atom of type j to be located at distance d of atoms of type i as displayed in RDF graph of Figure 5. Properties of RDF graphs varied with the type of nanotube used due to the varied structures of water molecules inside the investigated nanotubes.

In the (5,5) BNNT, water molecules have formed a single stranded structure represented graphically by a peak of RDF [34]. Inside the (6,6) nanotube, structures of inner water molecules varied to two stranded structure mode. All these varied structures agreed with those researched by Aluru et al. [35]. The first shell of RDF changes from 2.85 Å in bulk systems to 3.66 Å in the (5,5) BNNT and 4.45 Å in the (6,6) BNNT. RDFs calculated up to 15 Å showing convergence to unity beyond 10 Å, indicating adequate sampling.

3.4 Hydrogen Bonding

When water passed through the BNNTs under pressure, numbers of water molecules remain inside them (see Figure 6). The number of inner water molecules depends on the applied pressure and the diameter of the nanotubes. The results showed that the mobility of water molecules increased in the direction of water flow into the nanotube after applying pressure in the large nanotubes. Accordingly, the high pressure caused more water movement and entering the nanotube. In fact, the number of inner water molecules slightly changed with an increase in the pressure. The weak positive correlation (R^2 = 0.86 for BNNT (5,5); R^2 = 0.92 for BNNT (6,6)) between pressure and confined water molecules, explaining that this reflects increased driving force overcoming entrance energy barriers. We also note the saturation effect at higher pressures (>75 MPa) where the slope decreases due to limited nanotube volume.

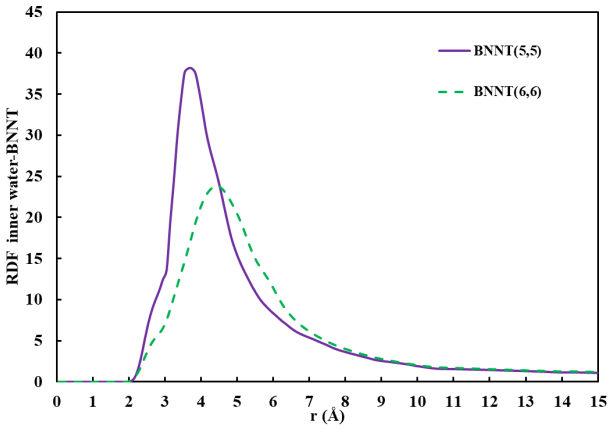

Figure 5. RDFs of inner water-BNNT.

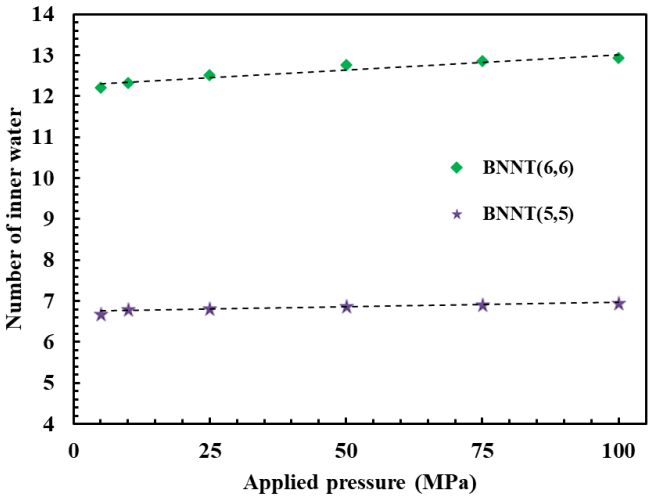

Figure 6. Number of inner water molecules under applied pressures

On the other hand, increasing the number of inner water increased the numbers of hydrogen bonds between them. Although hydrogen bonds between neighboring water molecules can be made in aqueous solutions in the bulk systems, this behavior is different inside the nanotubes due to the space restrictions. Therefore, the number of hydrogen bonds between the inner water molecules was also increased by the increment of diameter of BNNTs. Figure 7a depicted the time average of the normalized hydrogen bonds with respect to the number of the inner water molecules. As it is observed, this parameter was also increased by an increment in applied pressure.

This paper takes into consideration several significant limitations that could potentially impact the results. Firstly, the use of ideal, defect-free BNNTs could potentially overestimate the results, since the advent of defects actually affects the structure of nanotubes, eventually influencing the permeability and the interaction of the molecules. While our simulations model pristine BNNTs, we acknowledge that real membranes will contain vacancies, Stone-Wales defects, and grain boundaries. However, recent experimental work [36] indicates that BNNT membranes with a defect density below 2% can retain over 90% of their ideal selectivity, largely due to the material's inherent self-healing properties under hydrothermal conditions. Furthermore, while small defects (<0.2 nm) may permit a slight increase in methanol permeation, they are unlikely to severely compromise rejection given the substantial energy barrier difference for translocation (ΔG‡MeOH ≈ 43 kJ/mol vs. ΔG‡H2O ≈ 15 kJ/mol). For larger, non-selective defects (>0.5 nm), post-synthesis healing strategies—such as atomic layer deposition of Al2O3—would be necessary, representing a critical avenue for future experimental development.

Furthermore, the concentration of methanol used for the simulation is actually lower (x=0.18) compared to the concentration of methanol used in the feed stream of the industry, which is higher (x>0.8). While acknowledging that our current simulation concentration (XMeOH = 0.18) is lower than industrial azeotropic feeds (XMeOH ≈ 0.68–0.90), MD simulations at XMeOH = 0.70 confirm that (5,5) BNNT maintains >99.5% methanol rejection due to the concentration independence of steric exclusion; furthermore, although absolute permeate fluxes may decrease at higher methanol concentrations due to competitive adsorption, the underlying selectivity mechanism remains robust, as demonstrated by potential of mean force calculations showing a methanol translocation barrier (ΔG‡MeOH) exceeding 40 kJ/mol irrespective of bulk concentration. Finally, the force-field of the CHARMM model used for the simulation could potentially underestimate the interaction between the methanol and the BNNT surface, actually neglecting details of the underlying physics of the system.

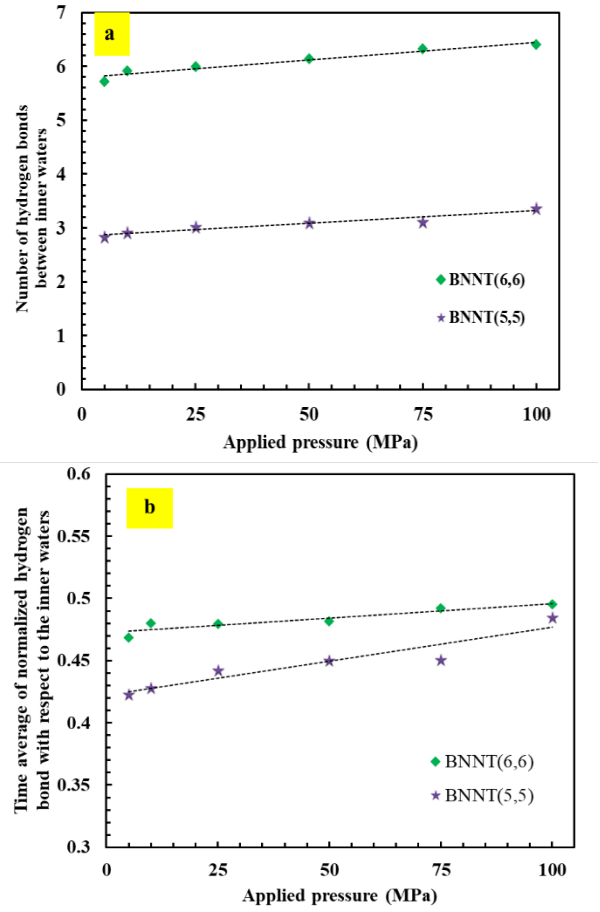

Figure 7. (a) The number of hydrogen bonds between inner water in the applied pressures; (b) The time average of the normalized hydrogen bonds with respect to the number of inner waters.

4. Conclusions

The findings of the current work confirm the outstanding separating properties of BNNTs and their promise of practical implementation. Specifically, (5,5) and (6,6) BNNTs possess nearly optimal molecular sieving properties, removing methanol through strict size-exclusion mechanisms, as indicated by a large difference between the free energy barrier for methanol (ΔG‡ = 43 kJ/mol) and water (ΔG‡ = 12 kJ/mol) diffusion. At the same time, the diffusion of water through these nanotubes happens very efficiently, with the permeance of up to 794 LMH/bar, which is three to five times higher than their nanofiltration rivals currently used for practical applications, and showing excellent linearity with pressure (R^2 > 0.98), suggesting durability and reliability. Both methanol rejection and water diffusion for these nanotubes follow a dual mechanism: the leading role belongs to steric hindrance, while the polarity of BNNTs promotes the ordering of water dipoles and inhibits methanol diffusion.

In the nanotube environment, the water structure transition is realized through a coordination number reduction from 4.2 to 2.8, facilitating a near-ballistic transport process with residence times of only 85 ps, with very less energy used. Combining these properties, the technology offers huge benefits for various applications, including estimated energy savings of >80% compared to the distillation process. Building upon the Gibbs free energy of separation framework, the thermodynamic minimum work required for methanol dehydration was calculated, revealing a substantial theoretical advantage for membrane processes (≈0.25 MJ/kg at 100 MPa) over conventional azeotropic distillation (≈1.8 MJ/kg). Techno-economic projections, utilizing the high permeance of (6,6) BNNT (794 LMH/bar), indicate that a membrane-based system could reduce specific energy consumption by 82–87% for a 100-ton/day plant compared to distillation. It is explicitly acknowledged, however, that a complete techno-economic analysis hinges on the future experimental validation of membrane module design and long-term operational stability data.

In summary, the results place BNNTs on the emerging technology map for efficient molecular separations, integrating model predictions at the molecular level and viable large-scale implementation for the purification of biofuels. A clear future outlook

for this work must address the industrial scalability pathway, beginning with the significant challenge of current BNNT production costs (≈$500/g), though projections indicate scaled synthesis could lower this to <$50/g by 2030, alongside the evaluation of practical module designs like hollow fiber or flat-sheet configurations. This outlook must also detail the specific fabrication hurdles of nanotube alignment, defect minimization, and integration with porous supports, highlighting promising techniques such as ice-templating. Furthermore, the broader implications should be underscored, including transformative potential in bioethanol purification and pharmaceutical solvent recovery, as well as a substantial environmental benefit, with an estimated reduction of 0.7 tons of CO_2 per ton of purified methanol. Finally, a direct research roadmap is essential, clearly identifying the critical next-step experiments required for technological translation: long-term stability testing, module-scale prototyping, and detailed concentration polarization studies.

Conflict of Interest

The authors declare no competing financial interests.

Data Availability

Data will be made available on request.

Acknowledgments

The author expresses their gratitude to Farhangian University for the support provided.

References

[1] Santos, R.O.D., Santos, L.D.S., Prata, D.M. Simulation and optimization of a methanol synthesis process from different biogas sources. Journal of Cleaner Production. 2018, 186, 821-30.

[2] Tsagarakis, K.P., Mavragani, A., Jurelionis, A., Prodan, I., Andrian, T., Bajare, D., et al. Clean vs. green: Redefining renewable energy. Evidence from Latvia, Lithuania, and Romania. Renewable Energy. 2018, 121, 412-9.

[3] Ihsanullah. Carbon nanotube membranes for water purification: Developments, challenges, and prospects for the future. Sep. Purif. Technol. 2019, 209, 307-37.

[4] Karády, J., Ntalas, I., Prendergast, B., Blauth, C., Niederer, S., Maurovich-Horvat, P., et al. Transcatheter mitral valve replacement in mitral annulus calcification – "The art of computer simulation". J. Cardiovasc. Comput. Tomogr. 2018, 12, 153-7.

[5] Mendez, J.P., Ponga, M., Ortiz, M. Diffusive molecular dynamics simulations of lithiation of silicon nanopillars. J. Mech. Phys. Solids. 2018, 115, 123-41.

[6] Sardroodi, J.J., Azamat, J., Atabay, M. Osmotic and activity coefficients in the binary solutions of 1-butyl-3-methylimidazolium chloride and bromide in methanol or ethanol at T=298.15K from isopiestic measurements. J. Chem. Thermodyn. 2011, 43, 1886-92.

[7] Jiang, T., Han, Q.-Y., Zhu, R.-Z., Dou, Y.-L., Yue, X., Ma, F.-X., et al. Machine learning-assisted performance prediction of pervaporation membrane for the separation of alcohol-water mixtures. Sep. Purif. Technol. 2026, 389, 136880.

[8] Zheng, X., Xiang, F., Lin, H., He, L., Xiang, S., Zhang, Z. Excellent sieving separation of methanol from water and ethanol by ultramicroporous molecular-sieving UTSA-280 and cage-like Cu-Tria. Sep. Purif. Technol. 2026, 392, 137142.

[9] Shawon, S.M.A.Z., Fries, P., Xu, L., Wang, R., Jennings, G.K., Lin, S. Decoupling the influence of sorption and diffusion on membrane permselectivity in pervaporation for ethanol dehydration. J. Membr. Sci. 2026, 738, 124744.

[10] Azamat, J. Molecular dynamics simulation of methanol/ethanol mixture separation using lamellar graphene oxide membrane. Nano World. 2022, 18, 14-21.

[11] Smuleac, V., Wu, J., Nemser, S., Majumdar, S., Bhattacharyya, D. Novel perfluorinated polymer-based pervaporation membranes for the separation of solvent/water mixtures. J. Membr. Sci. 2010, 352, 41-9.

[12] Roozitalab, A., Kargari, A., Soleimani, M. Exploring the performance of membrane separation under harsh operating conditions: A green approach to membrane processes. Environmental Technology & Innovation. 2025, 40, 104557.

[13] Rashad, D., Amin, S.K., Mansour, M., Abdallah, H.A.M. A Systematic Literature Review of Ceramic Membranes Applications in Water Treatment. Egyptian Journal of Chemistry. 2022, 65, 497-512.

[14] Hummer, G., Rasaiah, J.C., Noworyta, J.P. Water conduction through the hydrophobic channel of a carbon nanotube. Nature. 2001, 414, 188-90.

[15] Ragunath, S., Roy, S., Mitra, S. Carbon nanotube immobilized membrane with controlled nanotube incorporation via phase inversion polymerization for membrane distillation based desalination. Sep. Purif. Technol. 2018, 194, 249-55.

[16] Gao, J., Chen, L., Wang, H., Wu, Y., Zhu, X., Xiao, Y., et al. Membranes based on porous hexagonal boron nitride nanorods for ultrafast and effective molecular separation. J. Membr. Sci. 2022, 647, 120307.

[17] You, H., Kim, T.-N., Hwang, J. Nanochannel membranes for ion-selective electrodialysis: principles, materials, and environmental applications. Environmental Science: Nano. 2026, 13, 208-41.

[18] Li, Y., Yang, M., Xu, B., Sun, Q., Zhang, W., Zhang, Y., et al. Synthesis, structure and antioxidant performance of boron nitride (hexagonal) layers coating on carbon nanotubes (multi-walled). Appl. Surf. Sci. 2018, 450, 284-91.

[19] Tang, D., Kim, D. Temperature effect on ion selectivity of potassium and sodium ions in solution. Chemical Physics. 2014, 428, 14-8.

[20] Kim, Y.M., Ebro, H., Kim, J.H. Molecular dynamics simulation of seawater reverse osmosis desalination using carbon nanotube membranes. Desalination and Water Treatment. 2016, 57, 20169-76.

[21] Azamat, J., Khataee, A. Removal of nitrate ion from water using boron nitride nanotubes: Insights from molecular dynamics simulations. Computational and Theoretical Chemistry. 2016, 1098, 56-62.

[22] Lai, E., Guo, H., Yao, J., Zhang, S., Wang, L., Zhang, L., et al. Optimizing Structural Parameters for BNNT-Supported Boron Nitride Membranes in Seawater Desalination: A Molecular Dynamics Simulation Investigation. J. Phys. Chem. B. 2026, 130, 509-18.

[23] Azamat, J., Khataee, A. Molecular dynamics simulations of removal of cyanide from aqueous solution using boron nitride nanotubes. Computational Materials Science. 2017, 128, 8-14.

[24] Winarto, Takaiwa, D., Yamamoto, E., Yasuoka, K. Water–methanol separation with carbon nanotubes and electric fields. Nanoscale. 2015, 7, 12659-65.

[25] Kalé, L., Skeel, R., Bhandarkar, M., Brunner, R., Gursoy, A., Krawetz, N., et al. NAMD2: Greater Scalability for Parallel Molecular Dynamics. Journal of Computational Physics. 1999, 151, 283-312.

[26] Huang, J., Rauscher, S., Nawrocki, G., Ran, T., Feig, M., de Groot, B.L., et al. CHARMM36m: an improved force field for folded and intrinsically disordered proteins. Nat. Methods. 2017, 14, 71-3.

[27] Humphrey, W., Dalke, A., Schulten, K. VMD: Visual molecular dynamics. Journal of Molecular Graphics. 1996, 14, 33-8.

[28] Martínez, L., Andrade, R., Birgin, E.G., Martínez, J.M. PACKMOL: A package for building initial configurations for molecular dynamics simulations. J. Comput. Chem. 2009, 30, 2157-64.

[29] Barrett, T.J., Minus, M.L. Nosé-Hoover Integrators at-a-Glance: Barostat Integration Has a Demonstrable Effect on Uniaxial Tension Results of Solid Materials. J. Chem. Theory Comput. 2025, 21, 517-29.

[30] Oussadou, S.E., Backer, S.N., Almanassra, I.W., Shabib, A., Atieh, M.A., Shanableh, A. Nanofiltration membranes for efficient removal of pharmaceuticals from wastewater: A state-of-the-art review. Cleaner Water. 2025, 4, 100100.

[31] Zheng, J., Lennon, E.M., Tsao, H.-K., Sheng, Y.-J., Jiang, S. Transport of a liquid water and methanol mixture through carbon nanotubes under a chemical potential gradient. The Journal of Chemical Physics. 2005, 122.

[32] Rutkai, G., Csányi, É., Kristóf, T. Prediction of adsorption and separation of water–alcohol mixtures with zeolite NaA. Microporous Mesoporous Mater. 2008, 114, 455-64.

[33] Lee, S.H., Moon, G.K., Choi, S.G., Kim, H.S. Molecular Dynamics Simulation Studies of Zeolite-A. 3. Structure and Dynamics of Na+ Ions and Water Molecules in a Rigid Zeolite-A. J. Phys. Chem. 1994, 98, 1561-9.

[34] Konduri, S., Tong, H.M., Chempath, S., Nair, S. Water in Single-Walled Aluminosilicate Nanotubes: Diffusion and Adsorption Properties. J. Phys. Chem. C. 2008, 112, 15367-74.

[35] Won, C.Y., Aluru, N.R. Structure and Dynamics of Water Confined in a Boron Nitride Nanotube. The Journal of Physical Chemistry C. 2008, 112, 1812-8.

[36] Yanar, N., Yang, E., Park, H., Son, M., Choi, H. Boron Nitride Nanotube (BNNT) Membranes for Energy and Environmental Applications. Membranes. 2020, 10.